Progress In Electromagnetics Research C, Vol. 156, 169–174, 2025

PIER C

(Received 25 March 2025, Accepted 20 May 2025, Scheduled 8 June 2025)

A Compact Hybrid Multi-Notched UWB BPF Using Defected Microstrip Structure (DMS) and Short-Circuited Stub

Raaed Thaaban Hammed* and Hassan Saad Abdullah

Department of Electrical Engineering, University of Technology — Iraq, Baghdad, Iraq

ABSTRACT: In this letter, a compact passband filter with dual desirable attenuation narrow bands is developed for ultra-wideband application. Indeed, a grounded stepped impedance resonator in defected microstrip structure (GSIR-DMS) is realized with a specified high-pass cutoff frequency of (f_{GSIR}). Next, two cells of the designed GSIR-DMSs are cascaded to perform the proposed ultrawide passband filter. In addition, four $\lambda_g/4$ open-circuited stubs are inserted beside the GSIR-DMSs to create two transmission zeros (TZs) and improve the filter rejection performance. In order to suppress interference with some expected network channels, two desirable $\lambda_g/4$ short-circuited microstrip stubs are implemented and coupled to the body of the UWB filter. Finally, the filter is constructed, simulated, and measured using a Rogers-ceramic RO4360 substrate with a permittivity of $\varepsilon_r = 6.15$ and a thickness of $h = 1.016$ mm. The filter responses from measurement and simulation are compared and discussed. The produced filter is very small covering circuit area of about $(0.433\lambda_g \times 0.244\lambda_g)$ excluding the feeding ports.

1. INTRODUCTION

In 2002, the ultra-wideband (UWB) unlicensed frequency range 3.1 to 10.6 GHz with a low power transmission of −41 dBm was defined and released by the Federal Communication Commission (FCC) for commercial communication application [1]. Since then, many UWB filters have been designed and developed using different techniques and structures to achieve the FCC regulation with high characteristic specifications such as compactness, low insertion loss, high selectivity, and wide stopband rejection [2–10]. Filters with compact size are very well constructed in [2] using multilayered grounded E-shaped microstrip structure. Also, highly compact filters with ultra-broadband responses are deeply studied and implemented based on a hybrid of tapered/DGS in [3] and using queen-mode resonator in [4]. In order to enhance the filtering characteristic performance, [5–7] propose UWB filters with wide-stopband characteristic based on substrate integrated defected ground structure (DGS), superconducting quintuple-mode resonator, and a free via-hole multimode resonator respectively. Moreover, highly selective UWB filters [8–10] are also investigated and improved following different techniques. To eliminate the possible interference of some wireless network signals, UWB filters are developed with notched band frequency response [11–16]. By adding two strip lines, a composite right/left handed UWB filter is realized with dual notched band [11]. Following multilayer microstrip technology, the development of dual- and quad-notched UWB filters is achieved in [12]. In another technique, [13–15] create two transmission zeros using a folded split ring resonator coupled to the feed line of a UWB filter. In addition, [16] finds that a folded split ring DGS is a good solution to generate two rejection bands inside the UWB filtering response.

In this article, a dual notched band UWB filter is designed and realized based on $\lambda_g/4$ GSIR in DMS. The UWB bandpass filter (BPF) is formed by cascading two cells of GSIR-DMSs. To improve the filter rejection performance, two transmission zeros are generated meeting the resonance condition of the two cells $\lambda_g/4$ open-circuited stubs added beside the GSIR-DMSs. Finally, this filter is developed with independent dual-notched band. To this end, a prototype of the proposed filter is manufactured, and its filtering responses is measured and compared with simulation results.

2. BASIC UWB BPF BASED ON DMS

The conductor layout of the suggested UWB BPF is denoted in Figure 1(a). The filter structure consists of two cells of grounded stepped impedance resonator designed in a defected microstrip structure (Figure 1(b)). Also the filter layout shows that there are four quarter-wavelength open circuit stubs around the GSIRs. Following the design principles in [17], the circuit of the GSIR-DMS (Figure 1(b)) is realized, and its input admittance is calculated as:

$$Y_{in} = Y_1 \frac{jY_1 \tan\theta_1 - jY_2 \cot\theta_2}{Y_1 + Y_2 \cot\theta_2 \tan\theta_1} \tag{1}$$

Let $Y_{in} = 0$, then the resonance condition can be defined as:

$$\tan\theta_1 \tan\theta_2 = \frac{Y_2}{Y_1} \tag{2}$$

$$\theta_T = (\theta_1 + \theta_2) \tag{3}$$

where Y_2/Y_1 and θ are the admittance ratio and the electric length of the proposed GSIR-DMS. To this end and for the

* Corresponding author: Raaed Thaaban Hammed (raaed.t.hammed@uotechnology.edu.iq).

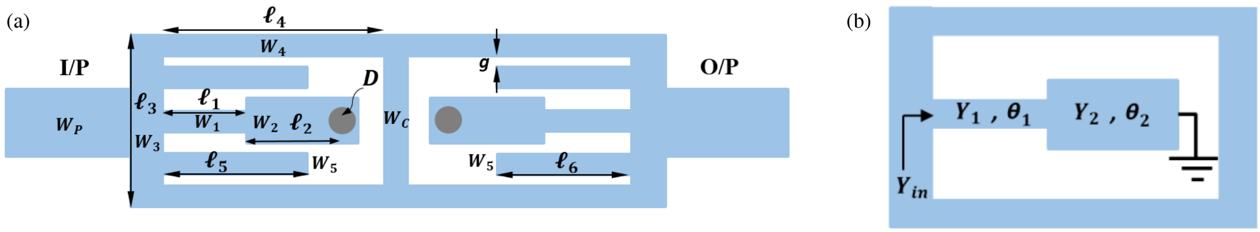

FIGURE 1. (a) Conductor pattern of the DMS UWB bandpass filter, and (a) Circuit of the GSIR-DMS.

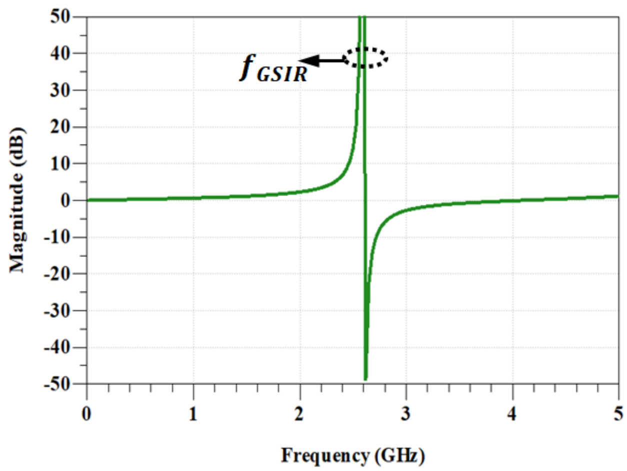

FIGURE 2. Frequency characteristic performance of the GSIR-DMS, Figure 1(b), in which $\ell_1 = 1.7$ mm, $W_1 = 0.3$ mm, $\ell_2 = 1.8$ mm, $W_2 = 0.7$ mm, $\ell_3 = 2.7$ mm, $W_3 = 0.5$ mm, $\ell_4 = 435$ mm, $W_4 = 0.3$ mm, and $W_P = 1.37$ mm.

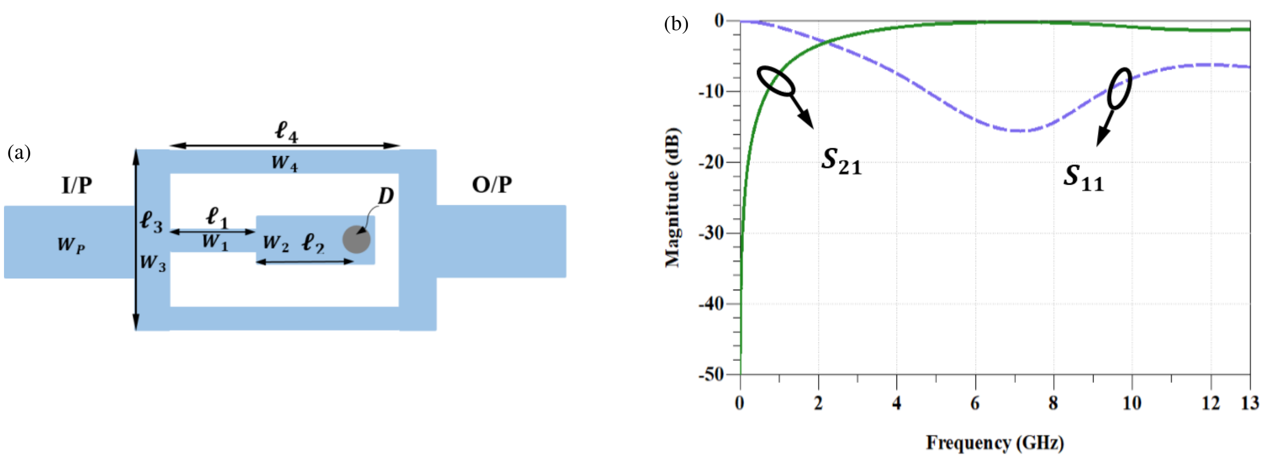

FIGURE 3. (a) Conductor pattern of the two-port GSIR-DMS with physical dimension as stated in Figure 2, and (b) its filtering response.

purposes of this work, a GSIR-DMS is realized with a high-pass cutoff frequency $f_{GSIR} = 2.58$ GHz. Using a substrate with a relative permittivity of $\varepsilon_r = 6.15$ and a thickness of $h = 1.016$ mm, the GSIR-DMS physical dimensions are computed, and its frequency characteristic is obtained in Figure 2. Obviously, the proposed structure can generate the desired resonance frequency. Connecting the proposed GSIR-DMS as a two-port network (Figure 3(a)), the filtering response of the structure is examined, and its result is reported in Figure 3(b). It is clear that the GSIR-DMS can provide a high-pass filtering behavior with a cutoff frequency close to f_{GSIR}.

Next, two of the designed GSRI-DMSs are cascaded and simulated to improve the expected UWB passband response (Figure 4(a)). The simulated S-parameter, Figure 4(b), shows that the introduced structure offers a bandwidth of 7.697 GHz with a poor upper rejection band. Note that these results are studied with a different W_C value of 0.6–0.3 mm in which $W_C = 0.3$ mm gives the best return loss. For the purposes of upper rejection band enhancement, two transmission zeros are created and coupled at 13 GHz and 14.5 GHz meeting the resonance frequency condition of the quarter-wave length open-circuited stubs. The physical dimensions and responses of the

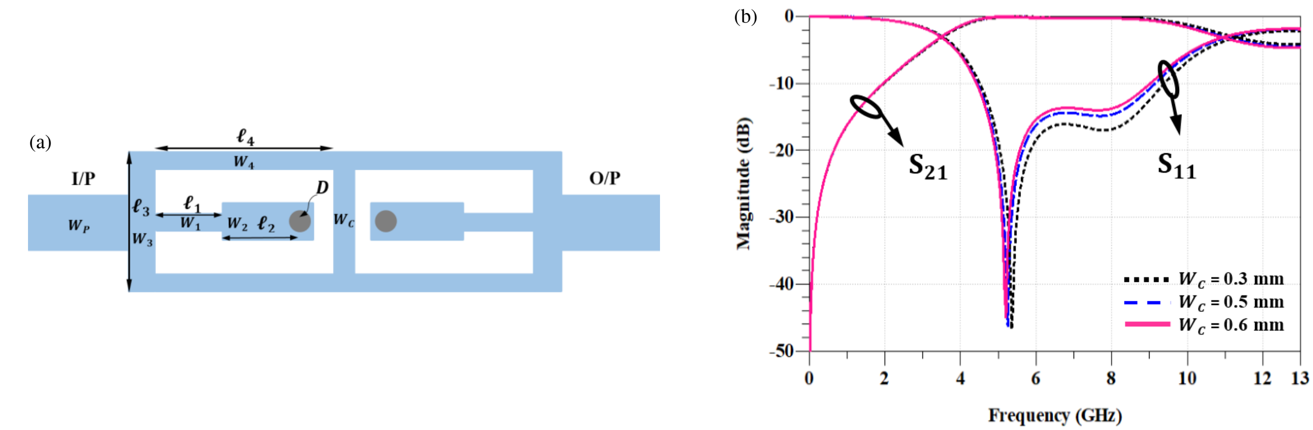

FIGURE 4. (a) Conductor pattern of two cascaded GSIR-DMSs, and (b) Its insertion and return losses with variable W_C values.

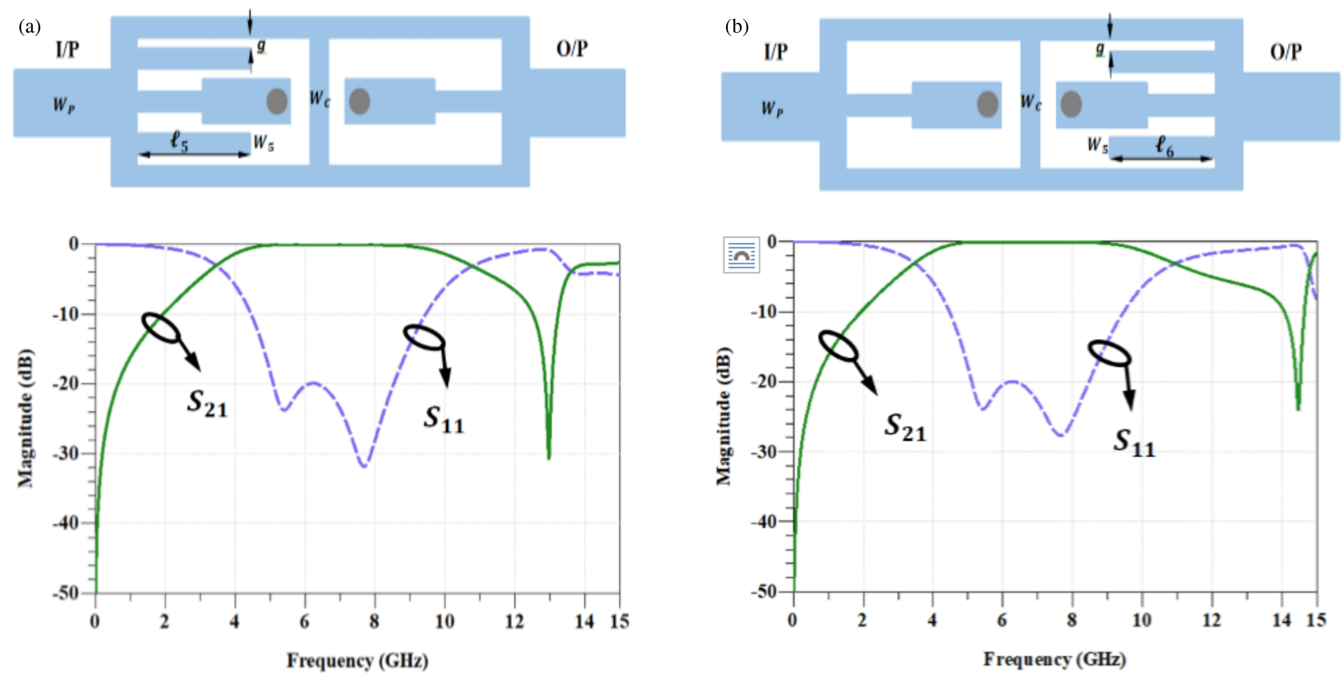

FIGURE 5. The UWB GSIR-DMS filter with four $\lambda_g/4$ open-circuited stubs designed at (a) 13 GHz meeting the physical dimensions of $\ell_5 = 2.7$ mm, $W_5 = 0.2$ mm, and $g = 0.25$ mm, and (b) 14.5 GHz meeting the physical dimension $\ell_6 = 24$ mm $W_5 = 0.2$ mm, and $g = 0.25$ mm.

TABLE 1. Physical dimensions of the GSIR-DMS UWB BPF, Figure 1(a).

Substrate	Lengths (mm)	Widths & Gaps (mm)
Rogers Ceramic RO4360 Dielectric constant $\varepsilon_r = 6.15$ Thickness $h = 1.016$ mm	$\ell_1 = 1.7$, $\ell_2 = 1.8$, $\ell_3 = 2.7$, $\ell_4 = 4.35$, $\ell_5 = 2.7$, $\ell_6 = 2.4$	$W_1 = 0.3$, $W_2 = 0.7$, $W_3 = 0.5$, $W_4 = 0.3$, $W_5 = 0.2$, $W_C = 0.3$, $W_P = 1.37$, $g = 0.25$.

filter with upper transmission zeros (13/14.5 GHz) are illustrated in Figures 5(a) and (b), respectively. Consequently, four desired $\lambda_g/4$ open-circuited defected microstrip stubs are designed and inserted besides the GSIR-DMSs as shown in Figure 1(a). To verify the above concept, the produced UWB filter, Table 1, is simulated, and its insertion and return losses are plotted in Figure 6(a). From this figure, the filter offers a low insertion loss about 0.06 dB around the center frequency 685 GHz and a return loss better than 20 dB. The upper rejection band is very well improved with two coupled TZs. The group delay is more or less 0.2 ns from 4.5 GHz to 8.5 GHz as shown in Figure 6(b). The filter has a compact size about 27 mm^2 excluding the input/output ports.

TABLE 2. A comparison between the proposed UWB filter and recently published works.

Ref.	IL (dB)	Notches (GHz)/ Attenuation (dB)	Passband (GHz)	RL (dB)	Circuit size $\lambda_g \times \lambda_g$
[11]	> 1	$4, 7/ > 14$	3.07–10.64	> 10	0.4×0.11
[13]	0.9	$6.1, 8.1/ > 15.5$	2.75–10.7	11	0.44×0.33
[14]	> 1	$5.8, 8/ > 14$	3.5–10.1	11	0.55×0.75
[15]	0.6	$6.8, 9.82/ > 26$	3.52–11.68	18	0.41×0.20
This work	**0.4**	$\mathbf{5, 7/ > 27}$	$\mathbf{2.9 - 10.4}$	$\mathbf{> 11}$	$\mathbf{0.43 \times 0.24}$

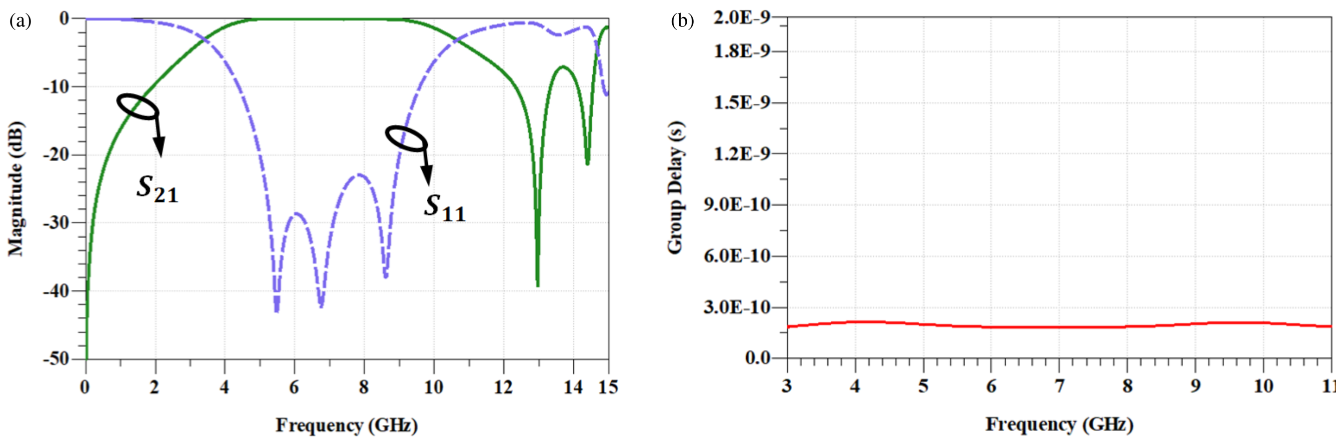

FIGURE 6. (a) The filtering attitude of the GSIR-DMS UWB bandpass filter, (see the filter in Figure 1(a)), and (b) its simulated group delay.

3. UWB FILTER WITH DUAL ATTENUATION NARROW BANDS

In Section 2, a new compact size UWB BPF with good filtering response specification is realized using DMS of GSIR and four parallel open circuited stubs. Due to the existence of the other wireless network signals allocated within the UWB bandwidth, the proposed filter is supported by two independent attenuation bands to suppress the expected interference (Figure 7). As shown in this figure, two $\lambda_g/4$ microstrip short-circuited stubs are analyzed and coupled to the body of the UWB filter through a coupling space S. In microwave principles, [17], the resonant behavior of the $\lambda_g/4$ microstrip short-circuited stub can be considered as a parallel LC-resonator. Based on coupling mechanism [18], the $\lambda_g/4$ grounded microstrip stub is transformed to a series resonant circuit between the input/output ports and the ground, producing a notch band. To examine the developed multi-notched UWB filter, Figure 7, two $\lambda_g/4$ grounded microstrip stubs are designed and coupled in which their physical dimensions and coupling distances are calculated to generate notch-1 at 5 GHz and notch-2 at 7 GHz. The simulated responses, Figure 8, show that the proposed technique can provide good stopband performance of 15 dB attenuation with narrow bandwidth of 74 MHz centered at 5 GHz and 114 MHz centered at 7 GHz.

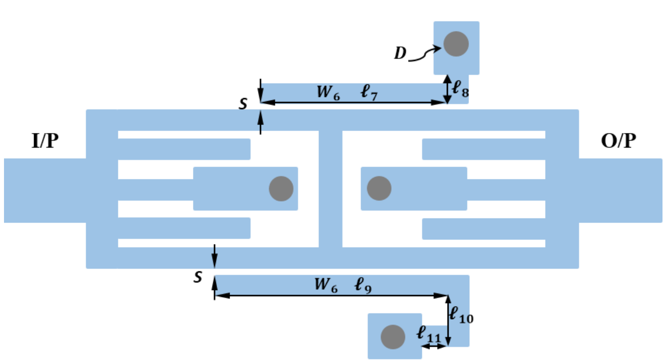

FIGURE 7. The planar dual-notched GSIR-DMS UWB filter using two $\lambda_g/4$ grounded microstrip stubs.

For experimental validation, the introduced multi-notched UWB passband filter, Figure 7, is manufactured with very compact size less than 56.5 mm^2 excluding the feeding ports Figure 9(a). In actual fact, a practical substrate of Rogers-Ceramic RO4360 with a dielectric constant of 6.15 and a thickness of $h = 1.016$ mm does not exist. Therefore, a double-layer technology is adopted in this work to produce the required thickness $h = 1016$ mm using two substrates of (Rogers (USA) Ceramic RO4360) with $h = 0.508$ mm. Using Anritsu MS4642A Vector Network Analyzer (VNA), the prototype is tested, and its responses are obtained and compared with the simulated results (Figure 9(b)). This figure shows good matching between the measured and simulated filtering results characterized by S-parameters. Reading the comparison carefully, the experimental filter offers a bandwidth from 2.9 to 10.4 GHz with an

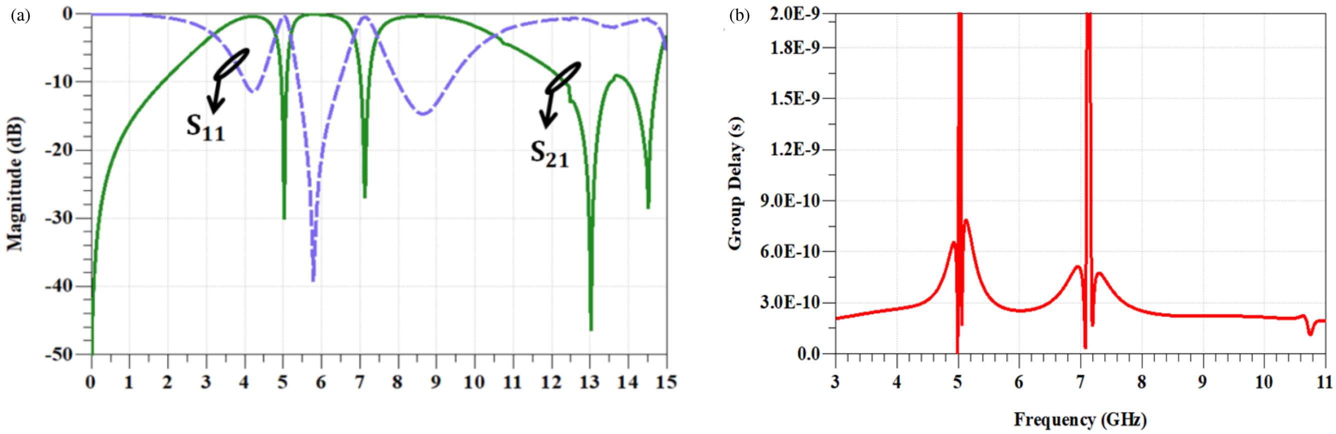

FIGURE 8. (a) The simulated insertion and return losses carried out from the dual-notched UWB GSIR-DMS filter, (see the filter in Figure 7), with $\lambda_g/4$ short-circuited stubs physical dimensions of $\ell_7 = 4.2$ mm, $\ell_8 = 0.5$ mm, $\ell_9 = 6.0$ mm $\ell_{10} = 0.8$ mm, $\ell_{11} = 0.4$ mm, $W_6 = 0.3$ mm, an $S = 0.2$ mm, and (b) Its group delay.

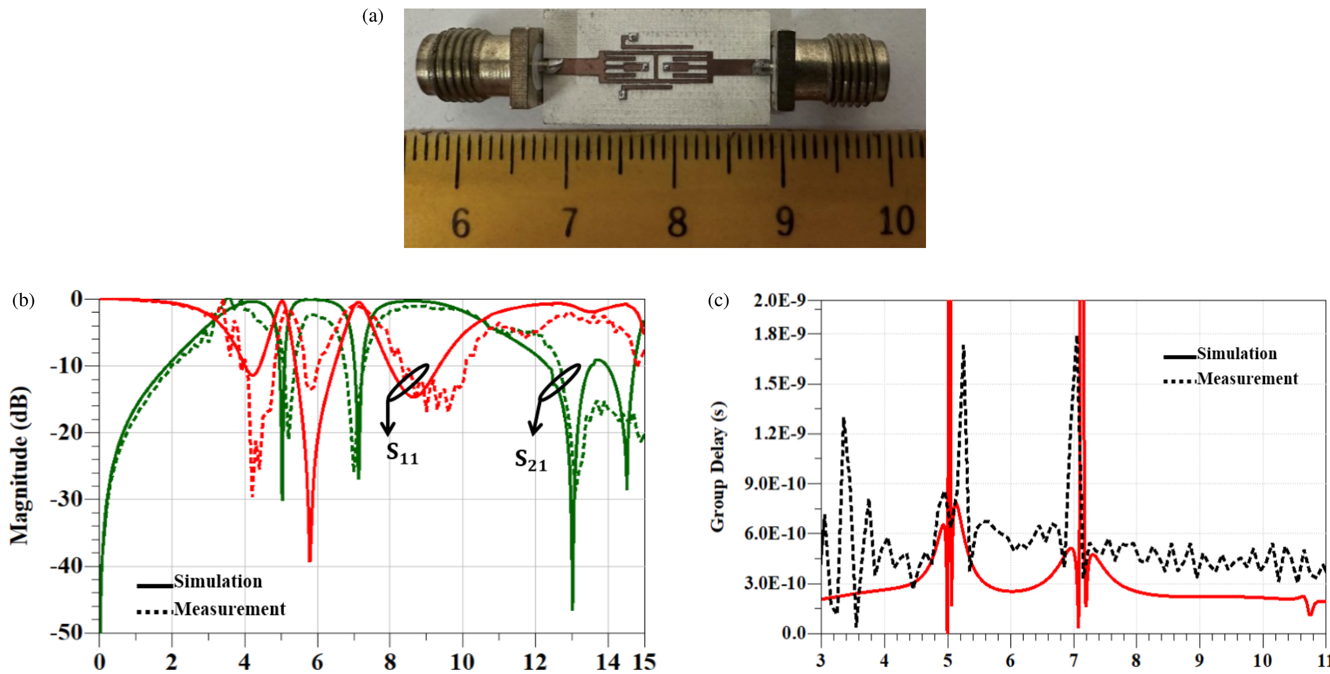

FIGURE 9. (a) Manufactured specified GSIR-DMS UWB filter with dual-notched bands. (b) Its S parameters from simulation and measurement, and (c) Its group delay.

insertion loss of less than 0.4 dB except the desired attenuation bands. The measured response, Figure 9(b), shows that the filter has two extremely narrow rejection bands from 5.14 to 5.29 GHz at 5 GHz and 6.867.15 GHz at 7.0 GHz with an attenuation value of 15 dB. Also, the filter has good roll of skirt selectivity with two favorite transmission zeros hence upper rejection band performance. The function of operation of the filter is also obtained through the group delay response as shown in Figure 9(c). Clearly, the filter has flat passbands of 0.2 ns group delay except the attenuated bands of 3 ns at 5 GHz and 1.6 ns at 7 GHz. In order to show the filter capability, a performance comparison with some recently reported works are summarized in Table 2.

4. CONCLUSION

A simple and virtual technique for producing two rejection notches in the passband of a compact UWB filter was presented in this article. In this technique two cells of GSIRs were realized and cascaded in a defected microstrip structure. For upper stopband enhancement, four quarter-wavelength open stubs were used and added to the filter structure. Moreover, two-notched narrow bands were remarkably generated using short-circuit stubs electrically coupled to the main filter. Finally, the simulated filter was fabricated, measured, and its results were compared and discussed. It is observed that the simulated and measured responses were in good agreement, and the filter has compact size.

REFERENCES

[1] Federal Communications Commission, "Revision of part 15 of the commission's rules regarding ultra-wideband transmission systems," First Report and Order FCC 02-48, 2002.

[2] Hammed, R. T. and D. Mirshekar-Syahkal, "Miniaturized high-order UWB bandpass filter using third-order E-shape microstrip structure," in *2012 IEEE/MTT-S International Microwave Symposium Digest*, 1–3, Montreal, QC, Canada, Jun. 2012.

[3] Sangam, R. S., S. Dash, and R. S. Kshetrimayum, "Ultra-broadband bandpass filter using linearly tapered coupled-microstrip line and open loop defected ground structure," *IEEE Transactions on Circuits and Systems II: Express Briefs*, Vol. 68, No. 1, 181–185, 2020.

[4] Shome, P. P. and T. Khan, "A quintuple mode resonator based bandpass filter for ultra-wideband applications," *Microsystem Technologies*, Vol. 26, No. 7, 2295–2304, 2020.

[5] Xie, J., D. Tang, Y. Shu, and X. Luo, "Compact UWB BPF with broad stopband based on loaded-stub and C-shape SIDGS resonators," *IEEE Microwave and Wireless Components Letters*, Vol. 32, No. 5, 383–386, 2021.

[6] Kong, Q., X. Lu, L. Zhou, R. Zhang, S. Zhou, B. Wei, and L. Jiang, "Design of superconducting ultra-wideband filter with wide stopband based on quintuple-mode resonator," *Electronics Letters*, Vol. 59, No. 18, e12958, 2023.

[7] Riaz, M., B. S. Virdee, P. Shukla, and M. Onadim, "Quasi-elliptic ultra-wideband bandpass filter with super-wide stopband," *AEU — International Journal of Electronics and Communications*, Vol. 105, 171–176, 2019.

[8] Hammed, R. T. and D. Mirshekar-Syahkal, "A compact high selectivity seventh-order UWB bandpass filter with ultra-stopband attenuation," in *2012 IEEE Radio and Wireless Symposium*, 135–138, Santa Clara, CA, USA, Jan. 2012.

[9] Danaeian, M., E. Zarezadeh, M. H. Gholizadeh, A.-R. Moznebi, and J. Khalilpour, "A compact and sharp rejection ultra-wideband bandpass filter based on short and open stub-loaded multiple mode resonators," *Journal of Electrical Engineering & Technology*, Vol. 15, No. 1, 469–476, 2020.

[10] Wei, G. Y., Y. X. Wang, J. Liu, Y. Gao, and X. T. Yao, "A novel highly selective UWB bandpass filter using quad-mode stub-loaded resonator," *Progress In Electromagnetics Research Letters*, Vol. 109, 57–63, 2023.

[11] Janapala, D. K. and M. Nesasudha, "A compact ultra wide band bandpass filter with dual band notch designed based on composite right/left-handed transmission line unit cell," *International Journal of RF and Microwave Computer-Aided Engineering*, Vol. 28, No. 9, e21569, 2018.

[12] Hammed, R. T., "Miniaturized high-order ultra-wideband bandpass filters with multiple band rejection notches," *Electromagnetics*, Vol. 35, No. 8, 538–549, 2015.

[13] Ghazali, A. N., M. Sazid, and S. Pal, "A miniaturized low-cost microstrip-to-coplanar waveguide transition-based ultra-wideband bandpass filter with multiple transmission zeros," *Microwave and Optical Technology Letters*, Vol. 62, No. 12, 3662–3667, 2020.

[14] Wei, G. Y., Y. X. Wang, J. Liu, Y. Gao, and X. T. Yao, "Highly selective UWB BPF with dual notched bands using split ring resonator," *Progress In Electromagnetics Research C*, Vol. 136, 51–60, 2023.

[15] Gao, M., Y. He, J. Nan, Z. Yang, and C. Wang, "A miniaturized ultra-wideband filter with high rejection and selectivity based on dual-notch bands," *PLoS ONE*, Vol. 19, No. 8, e0306730, 2024.

[16] Sazid, M. and N. S. Raghava, "Planar UWB-bandpass filter with multiple passband transmission zeros," *AEU — International Journal of Electronics and Communications*, Vol. 134, 153711, 2021.

[17] Jia-Sheng, H. and M. J. Lancaster, *Microstrip Filters for RF/Microwave Applications*, 235–272, John Wiley & Sond. Inc, New York, 2001.

[18] Hammed, R. T. and B. H. Hameed, "Compact multiple band-stop filter using integrated circuit of defected microstrip structure (DMS) and dual-mode resonator," *AEU — International Journal of Electronics and Communications*, Vol. 107, 209–214, 2019.